

Yudy Natalia Flórez  
David Moratal  
Juana Forner  
Luis Martí-Bonmatí  
Estanislao Arana  
Ulises Guajardo-Hernández  
José Millet-Roig

## Semiautomatic analysis of phase contrast magnetic resonance imaging of cerebrospinal fluid flow through the aqueduct of Sylvius

Received: 9 September 2005  
Accepted: 27 March 2006  
Published online: 9 May 2006  
© ESMRMB 2006

Y. N. Flórez · D. Moratal · J. Millet-Roig  
Grupo BET (Bioingeniería,  
Electrónica y Telemedicina),  
Universitat Politècnica de València,  
València, Spain

D. Moratal · J. Forner  
L. Martí-Bonmatí (✉) · E. Arana  
Resonancia Magnética,  
Servicio de Radiología, Clínica Quirón,  
Avda. Blasco Ibáñez, 14,  
46010 Valencia, Spain  
E-mail: Luis.Marti@uv.es

L. Martí-Bonmatí  
U. Guajardo-Hernández  
Hospital Universitari Dr. Peset,  
Valencia, Spain

**Abstract** *Objective:* Quantification of the cerebrospinal fluid (CSF) flow through the aqueduct of Sylvius by means of magnetic resonance imaging (MRI) is subject to interobserver variability due to the region of interest (ROI) selection. Our objective is to develop a semiautomatic measurement method to achieve reproducible quantitative analysis of CSF flow rate and stroke volume. *Material and methods:* MR examinations were performed using a 1.5 T scanner with a phase contrast sequence (velocity encoding [ $V_{enc}$ ] of 20 cm/s, FOV = 160, 3 mm slice thickness, image matrix size = 256 × 256, TR = 53 ms, TE = 11 ms, NSA = 2, flip angle = 15° and 23 frames per cardiac cycle with peripheral retrospective pulse gating). Our method was developed using MATLAB R7. Errors introduced by background offset and possible aliased pixels were automatically detected and corrected if necessary in order to calculate the flow parameters that characterize CSF dynamics. The semiautomatic seed method reproducibility was

evaluated and compared with the radius method by two observers analysing 21 healthy subjects.

*Results:* The measurements using the semiautomatic seed method reduced the interobservers variability (intra-class correlation [ICC] = 1.0 for stroke volume and for volumetric flow rate) versus the radius method (ICC = 0.46 for stroke volume and 0.65 for flow rate). Normal stroke volume ( $39.19 \pm 20.13 \mu\text{l}/\text{cycle}$ ), flow rate ( $3.81 \pm 2.81 \text{ ml}/\text{min}$ ), maximal mean systolic velocity ( $5.27 \pm 1.3 \text{ cm}/\text{s}$ ) and maximal mean diastolic velocity ( $4.20 \pm 1.4 \text{ cm}/\text{s}$ ) were calculated with the half moon and aliasing corrected seed method.

*Conclusions:* Semiautomatic measurements (seed method with half moon background and aliasing correction) allow a generalization of the calculus of flow parameters with great consistency and independency of the operator.

**Keywords** Aliasing correction · Cerebrospinal fluid · Magnetic resonance · Phase imaging · Segmentation algorithm

### Introduction

Flow disturbances in the cerebrospinal fluid (CSF) flow dynamic through the aqueduct of Sylvius have been pointed in relationship with normal pressure hydrocephalus. In order to analyse the behaviour of the CSF flow through the aqueduct of Sylvius, two types of analysis

are generally carried out: a qualitative analysis and a quantitative evaluation. A qualitative analysis allows a rapid evaluation but it is rarely used due to its inconsistencies and errors associated to the sequence parameters dependence [1].

Flow measurements with phase contrast MR imaging (PC-MRI) provide a powerful clinical tool for the non-invasive evaluation of flowing fluids. The broad

distribution of MR systems makes these measurements readily available to a large number of patients in many institutions [2]. However, analyses of PC-MRI measurements are subject to variability and inaccuracy. The manual segmentation of the aqueduct by drawing a region of interest (ROI) is one of the main sources of variability. The partial volume effect between parenchyma and CSF, the possible residual systematic errors caused by imperfect suppression of eddy currents or brain motion and the presence of aliasing are the main sources of inaccuracy. The accurateness of the measurements can be increased by minimizing the partial volume effects using thinner slices, smaller pixel sizes and an imaging plane perfectly perpendicular to the aqueduct [3–6]. Variability and inaccuracy generates artefactual measurements that are not representative of real values. Quantitative evaluation needs a definition of an adequate ROI for an optimal measure of the different flow parameters [7, 8]. Although most papers use a manually placed ROI to define the aqueduct, this approach gives large inaccuracies [9–11] justifying the development of computer assisted segmentation techniques. Several approaches to automatic or semiautomatic segmentation of PC-MR images have been described. Baledent et al. [12] developed a method to segment cerebrospinal fluid space using the Fourier transform of the velocity time series comparing the first harmonic with the mean flow to identify the oscillatory flow, Kozerke et al. [13] and Yuan et al. [14] used active contours for the automatic vessel segmentation, Box et al. [9] used a seed point to model the blood velocity profile, while Alperin and Lee [15] used the temporal and spatial information for lumen boundary identification and a cross-correlation threshold to increase measurement reproducibility. This latter method has been modified for the automatic segmentation of the aqueduct [16], but no specific validation has been published.

Our purpose was to develop an appropriate unified computer assisted quantification technique to study the flow characteristics of the CSF within the aqueduct. This method should be reproducible integrating a semiautomatic segmentation technique of the aqueduct of Sylvius with background phase correction and aliased pixels detection and correction, when necessary. The final results should express the different parameters that characterize the CSF flow (mainly mean flow, mean velocity and stroke volume). This tool should make MR measurements mostly independent of the observer and the MR acquisition, generalizing the calculus of MR flow parameters.

## Materials and methods

### Data acquisition

Twenty-one healthy subjects (10 men and 11 women) with a mean age of  $40.8 \pm 18.7$  years (range 3–70) were examined using a 1.5 T

unit (Gyrosan Intera MR scanner, Philips Medical Systems, Best, The Netherlands). A PC sequence in an oblique-transversal plane perpendicular to the aqueduct of Sylvius at its midpoint was obtained. Main image parameters included a gradient echo sequence with a fixed velocity encoding ( $V_{\text{enc}}$ ) of 20 cm/s, FOV =  $160 \times 160 \text{ mm}^2$ , 3 mm slice thickness, matrix size =  $256 \times 256$ , yielding an image resolution of  $0.62 \times 0.62 \times 3 \text{ mm}$  per pixel, TR = 53 ms, TE = 11 ms, NSA = 2, flip angle =  $15^\circ$  and 23 frames per cardiac cycle with use of peripheral pulse retrospective gating. Total scan time duration was 4 min and 33 s. This technique allowed flow velocities measurements throughout the whole brain cycle as described previously [17–20]. The shortest available repetition time (TR) was selected in order to optimize temporal resolution, and the shortest available echo time (TE) to optimize signal to noise ratio and to reduce intravoxel phase dispersion [6, 21–24].

The velocity encoding value was chosen just slightly greater than the maximum observed flow velocity in patients with normal pressure hydrocephalus so as to obtain accurate flow measurements and to avoid aliasing [11]. In this work, all individuals were healthy subjects and presented flow velocities around 5 cm/s. In our clinical MR protocol, the  $V_{\text{enc}}$  has a fixed value of 20 cm/s in order to avoid aliasing from any subject, being healthy or not.

### Data analysis

The method was developed using MATLAB R7 (The MathWorks, Inc., Natick, MA, USA) with a graphical user interface to facilitate its use.

Interobservers' measurement variations were evaluated as the most important way to analyse the reproducibility of the proposed method. Intraobservers variability was not evaluated in this work. To evaluate the interobservers' measurement variations, two observers made independent analysis with the radius and seed methods (described later) in every patient. The experiment was completed with the calculus of CSF flow parameters (volume per cycle or stroke volume, mean flow through the aqueduct adding both craniocaudal directions and mean systolic and diastolic velocities). To assess flow through the aqueduct of Sylvius, a laminar profile velocity was assumed, with the highest values located in the centre while velocity decreases as radius enlarges.

### Segmentation of the aqueduct of Sylvius

In the *radius method*, the ROI detection procedure is initiated manually. The observer selects, between the modulus or phase images, the image with the highest contrast between CSF and mesencephalon. The user marks two points: the first one will be the centre of the ROI and the second will determine its radius. Finally, this circular ROI is copied to all frames of the phase series.

The *semiautomatic seed method* procedure is manually initialized by selecting a seed point inside the aqueduct on the magnitude image [9]. The method creates a new mean working matrix

with an area of  $81 \text{ mm}^2$  around the seed in order to minimize computational burden. In this matrix, each pixel intensity reflects the mean intensity of the pixels all along the magnitude images sequence. The aqueduct, having a diameter smaller than  $4 \text{ mm}$  [11,25], will be surely contained in that  $81 \text{ mm}^2$  working area.

Within this new matrix, the method looks for the maximum intensity. All subjects were analysed using a threshold calculated as  $(I_{\max} - I_{\min})/2$ , where  $I_{\max}$  is the highest mean intensity and  $I_{\min}$  is the smallest mean intensity of the mean matrix. To reduce variability, a new mean matrix is created again, centred in the  $I_{\max}$  pixel, and to avoid any influence from vascular and CSF structures in the selection of the threshold, the  $I_{\min}$  value is chosen from the upper half of the matrix.

A binary working matrix is then constructed, based on the threshold value, thus minimizing the errors resulting from slow flow, phase noise and contribution of partial volume effect (PVE) [6,9,26]. This threshold will give reproducibility to the method.

From this binary working matrix, a ROI is defined as the boundary that contains the pixels with a velocity higher than the selected threshold. The ROI will then have a variable shape, depending on the subject. Figure 1 displays different ROIs calculated for different subjects.

### Background correction

Flow studies are prone to systematic errors caused by imperfect suppression of eddy currents or brain motion [3,5]. The main source of error is the null background offset due to long term eddy currents, which varied less along the phase encoding than along the frequency encoding direction [4].

To correct these possible residual systematic errors we measured an average value of offset per frame in background baseline regions where brain motion is minimal or absent during the cardiac cycle in order to subtract this value from the apparent velocities in the ROI. As data filtering is not introduced in the reconstruction of the phase maps by the manufacturer's software, a background correction method must be implemented. This correction factor is calculated from the ROI surrounding mid-brain tissue [3,5,6,10]. The measures with correction and without correction will be analysed.

The value of offset for background correction is calculated from a ROI surrounding tissue or midbrain. A *half moon* region is automatically selected surrounding the upper part of the ROI, where the *half moon* region inner radius equals  $4R_{\text{ROI}}$  and the outer radius equals  $6R_{\text{ROI}}$ , being  $R_{\text{ROI}}$  an hypothetical ROI radius calculated as half the diameter of the ROI in the horizontal direction. We have used a *half moon* region instead of a *full moon* region because this assures a parenchymal location avoiding any partial volume from vascular and cistern structures.

For the *midbrain* region, the observer selects a point in the midbrain. A circular ROI will then be formed with  $42 \text{ mm}^2$  area using that selected point as its centre (Fig. 2). This ROI area assures us to correctly determine the value that will be applied for background correction.

### Aliasing correction

The presence of aliased pixels in the aqueduct through the sequence of images depends on the adequacy of the  $V_{\text{enc}}$  value chosen at the moment of the MR acquisition. The most accurate flow measurements are obtained when the  $V_{\text{enc}}$  is just slightly greater than the maximum observed flow velocity. However, in some pathologic cases with high flow rates, the selected  $V_{\text{enc}}$  is inadequate [21,23].

In order to detect aliased pixels, the first step of our method consists in detecting the frames within the sequence with presence of aliased pixels. To achieve this, the trend of the CSF movement through the aqueduct of Sylvius has to be determined for pixels with maximum and minimum values, thereby calculating the standard deviation of the neighbouring pixels. If the pixels have a value smaller than three standard deviations, it is assumed that there are no aliased pixels within that frame.

After selecting the frames with aliasing, the aliased pixels were identified by choosing the pixels with values higher than  $V_{\text{enc}}/10$  or smaller than  $-V_{\text{enc}}/10$  depending on the trend of the motion flow (if the trend is negative the considered aliased pixels are those with a value higher than  $V_{\text{enc}}/10$  and if it is positive, those with a value smaller than  $-V_{\text{enc}}/10$ ). In this way an important reduction of the computational burden is achieved because a low number of pixels will be analysed.

The new velocity value of the aliased pixel is obtained from Eq. (1):

$$V_{\text{AliasedPixel}} = \left(2V_{\text{enc}} - |V_{\text{pixel}}|\right) \left(\frac{-|V_{\text{pixel}}|}{V_{\text{pixel}}}\right), \quad (1)$$

where  $V_{\text{pixel}}$  represents the absolute velocity value measured in the aliased pixel [12].

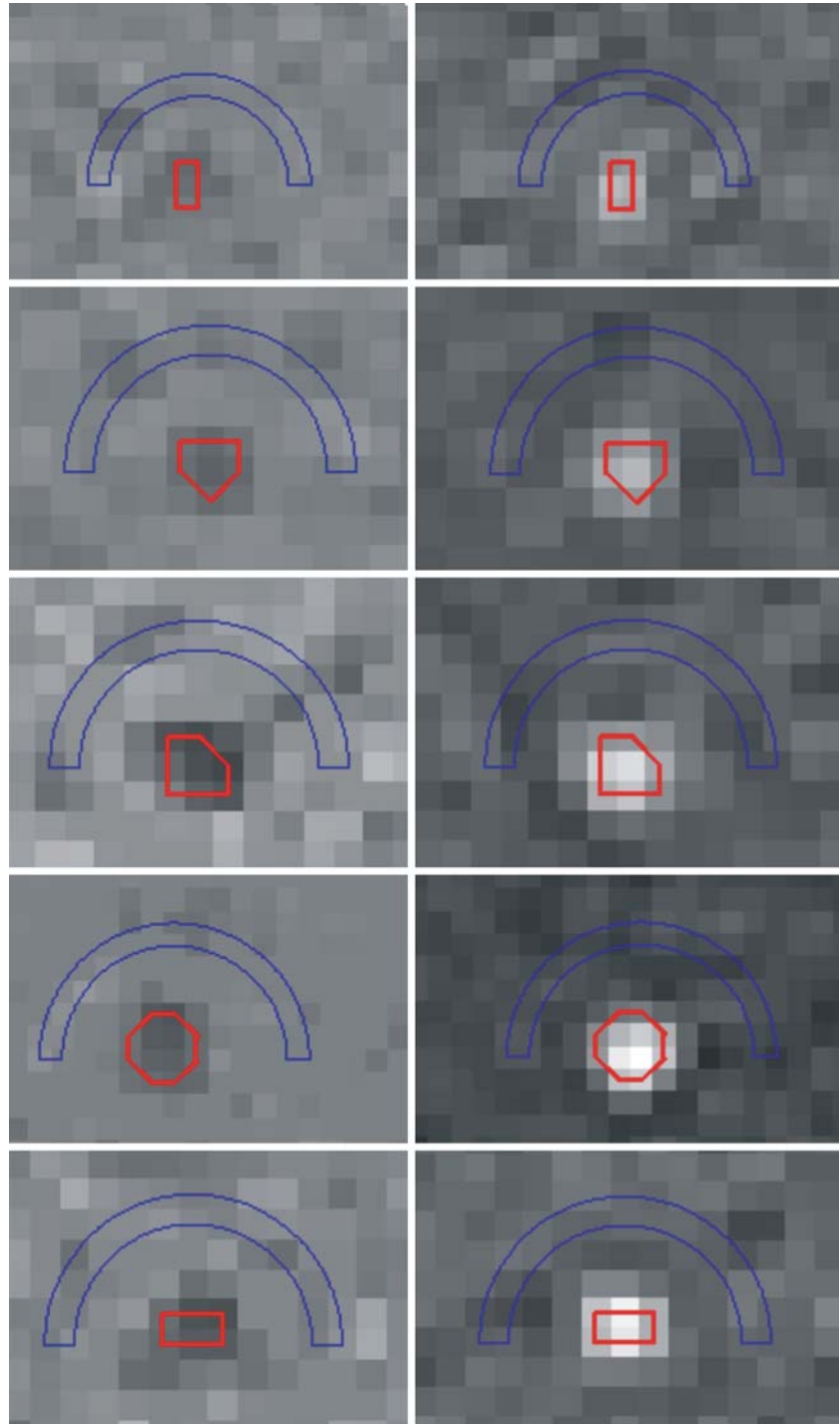
So, the aliased pixels are automatically detected and corrected, if necessary, throughout the whole sequence. This process is automatically applied without the user intervention. A 3D visualization of the movement of the CSF through the aqueduct allows a visual analysis of the aliasing correction. Figure 3 shows a PC frame before and after the aliasing correction.

### Quantitative analysis

The flow rate (ml/s) through the aqueduct is obtained as the product of the average velocity (cm/s) within the region by the ROI area ( $\text{cm}^2$ ). The stroke volume or volume per cycle is defined as the volume of fluid moving craniocaudally during systole and opposite during diastole. The stroke volume is calculated integrating the area under the volumetric flow rate curve over a cycle. The mean of the absolute value of these two measurements is the volume per cycle [5]. This parameter is used as predictor in normal pressure hydrocephalus for pre- and post-shunt therapy [5].

The calculated values of the flow velocity are plotted against time with a cubic spline interpolation of the last and first values of the cycle [5,16,27].

**Fig. 1** Different ROI shapes determined through a seed point. *Left column* ROI on phase images. *Right column* ROI on magnitude images



#### Statistical analysis

The agreement of the measurement methods was investigated using the method of Bland and Altman [28], standard deviation, intra-class correlation (ICC) and systematic difference (sys diff). This last parameter is defined as the difference between the mean

values obtained for every parameter using every method for two observers.

The ICC value allows evaluating the agreement level between the measurements obtained by two observers. An ICC value  $> 0.90$  is very good,  $0.71-0.90$  is good,  $0.51-0.70$  is acceptable,  $0.31-0.50$  is insufficient and  $< 0.30$  is poor [29,30].

**Fig. 2** Background correction. *Left* half moon surrounding the ROI. *Right* midbrain ROI manually placed

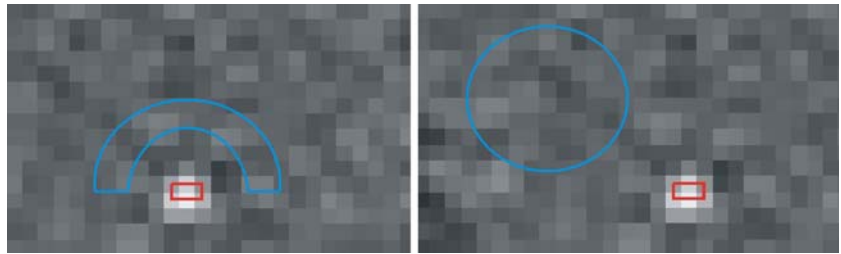


**Fig. 3** *Left* frame with presence of pixels with aliasing. *Right* same frame after applying an aliasing correction. In order to show the aliasing correction, the velocity encoding value for this acquisition was 10 cm/s, because in this work, all the data belongs to healthy subjects (with flow velocities around 5 cm/s). The protocol in our study considers a systematic velocity encoding of 20 cm/s in order to avoid aliasing for every kind of patient

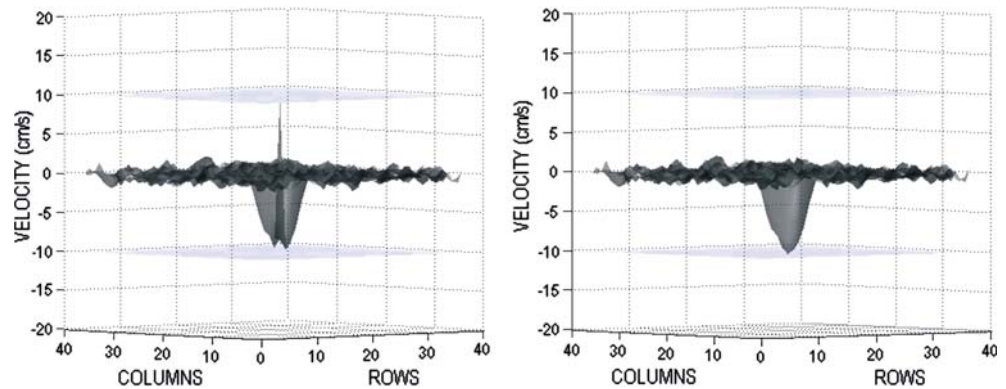


**Table 1** Interobserver's variability using the *seed method* to define the ROI and applying different background corrections

	Mean (SD)	Mean (SD)	ICC (95% rel)	Sys diff	Sig
	Observer 1	Observer 2			
Stroke volume ( $\mu\text{l}/\text{cycle}$ )					
C. half moon	39.19 (20.13)	39.19 (20.13)	1.00 (-1.00,1.00)	0.0	1.00
C. midbrain	38.19 (18.55)	38.25 (18.53)	1.00 (-0.99,1.00)	0.06	0.99
No correction	40.83 (20.09)	40.83 (20.09)	1.00 (-1.00,1.00)	0.0	1.00
Mean flow (ml/min)					
C. half moon	3.81 (2.17)	3.81 (2.17)	1.00 (-1.00,1.00)	0.0	1.00
C. midbrain	3.71 (2.00)	3.71 (2.01)	1.00 (-0.99,1.00)	0.0	0.99
No correction	3.96 (2.17)	3.96 (2.17)	1.00 (-1.00,1.00)	0.0	1.00

ICC intra-class correlation, *Sys diff* systematic difference

ANOVA test was used to compare the values obtained with background correction and no correction. Null hypotheses were verified using a 2-sided test and  $p$  values smaller than 0.05 were considered significant.

The influence of sex and age on volume and flow measurements was evaluated with the Student  $t$  test for independent samples and the ANOVA Student–Newman–Keuls test for multiple groups (age categorized as < 25, 26–50, 51–75 years old).

## Results

A semiautomatic measurement method that achieves reproducible quantitative analysis of CSF flow has been developed. Our seed method was compared with the radius method and the interobservers' variability was evaluated.

The measurements carried out by two observers using the radius method showed much higher interobservers variability than the measurements carried out by the same observers using our seed method. The mean flow, stroke volume, standard deviation, ICCs and systematic differences for both methods are presented in Tables 1 and 2. The ICCs indicate that the reproducibility was significantly better with the seed method than with the radius method.

Figures 4, 5 and 6 plots the interobserver variability of the measurements using the seed method either without correction, with half moon and with midbrain correction using the Bland and Altman method. There was considerable agreement between the two observers using the seed method for every flow and stroke registry, with half moon, midbrain offset correction and no correction.

**Table 2** Interobserver's variability using the *radius method* to define the ROI and applying different background corrections

	Mean (SD) Observer 1	Mean (SD) Observer 2	ICC (95%)	Sys diff	Sig
Stroke volume ( $\mu$ l/cycle)					
Half moon correction	27.56 (16.53)	21.90 (9.66)	0.46 (−0.078,0.736)	5.66	0.072
Midbrain correction	28.03 (17.18)	22.08 (9.43)	0.45 (−0.063,0.728)	5.95	0.068
No correction	30.49 (18.17)	23.66 (9.71)	0.40 (−0.019,0.702)	6.38	0.055
Mean flow (ml/min)					
Half moon correction	1.47 (0.78)	1.51 (0.59)	0.65 (−0.320,0.846)	0.04	0.750
Midbrain correction	2.08 (1.54)	1.54 (0.59)	0.43 (−0.042,0.716)	0.54	0.054
No correction	1.63 (0.87)	1.65 (0.62)	0.60 (−0.237,0.819)	0.02	0.905

ICC intra-class correlation, *Sys diff* systematic difference

However, the method presented more dispersion when midbrain correction was used.

The ANOVA test did not show statistical differences among the two background corrections and without correction for neither stroke volume ( $F: 0.97, p = 0.90$ ) nor mean flow ( $F: 0.79, p = 0.92$ ).

The measures obtained for stroke volume and for mean flow using our seed method with correction of half moon were  $39.19 \pm 20.13 \mu\text{l/cycle}$  and  $3.81 \pm 2.17 \text{ ml/min}$ , respectively. The measures obtained in our study with correction of half moon were  $5.27 \pm 1.3 \text{ cm/s}$  for the maximal mean systolic velocity and  $4.20 \pm 1.4 \text{ cm/s}$  for the maximal mean diastolic velocity.

Using the seed method with the half moon correction, we have found that sex did not statistically influence CSF values (stroke volume:  $38.03 \pm 22.86$  and  $40.71 \pm 17.01$ ,  $F = 0.09, p = 0.78$ , female and male, respectively; mean flow:  $3.79 \pm 2.77, 3.82 \pm 1.11$ ,  $F = 0.01, p = 0.98$ , female and male, respectively). Age also had no statistically significant influence on these measurements (stroke volume: < 25 years old,  $56.13 \pm 1.55 \mu\text{l/cycle}$ ; 26–50 years old,  $39.41 \pm 25.23 \mu\text{l/cycle}$ ; 51–75 years old,  $31.55 \pm 8.79 \mu\text{l/cycle}$ ,  $F = 1.67, p = 0.21$ ; mean flow: < 25 years old,  $6.17 \pm 1.83 \text{ ml/min}$ ; 26–50 years old,  $3.61 \pm 2.43 \text{ ml/min}$ ; 51–75 years old,  $3.09 \pm 1.12 \text{ ml/min}$ ,  $F = 2.53, p = 0.107$ ).

## Discussion

Our results demonstrate that the agreement level obtained with the radius method (ICC = 0.46) is insufficient, while the seed point method provides a very good agreement level (ICC = 1.00). With this latter method, the variability was eliminated in its totality. The greater reliability for the seed method is due to the way the ROI is selected.

A highly reproducible method is needed in the evaluation of CSF flow dynamic abnormalities within the aqueduct of Sylvius. From our results it can be concluded

that our semiautomatic seed method resulted to be highly reproducible.

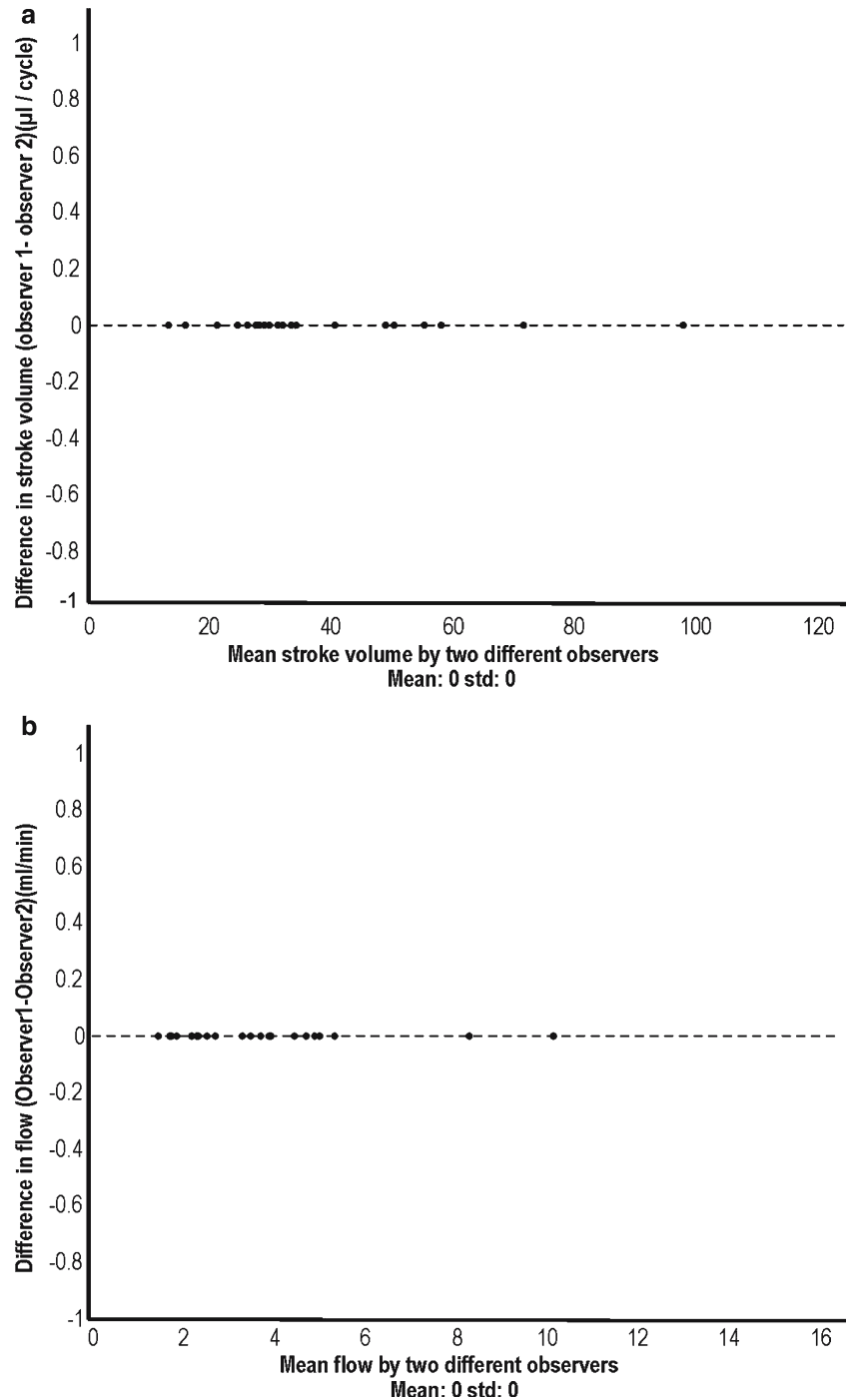
There have been proposed previous threshold based CSF segmentation methods [12, 15]. Baledent et al. [12] visually selected a threshold applied to a parametric image in which the pixel intensity depended on the magnitude of a fundamental frequency of the CSF Fourier analysis. Alperin and Lee [15] in his pulsatility-based segmentation technique selects a reference velocity waveform, generating a cross-correlation (CC) map and then, computing a CC threshold value. Once this threshold value has been selected, the boundary of a region containing connected pixels with values above this threshold is obtained.

In [12], Baledent et al. apply an aliasing correction to those visually detected aliased pixels. In [27], Baledent et al. apply a background correction manually selecting a ROI in the adjacent tissues of the aqueduct. In our proposed method all the entire sequence is analysed, automatically detecting any aliased pixels and correcting it if necessary and automatically selecting a *half moon* region to background correction.

Previous studies have used background baseline regions (which represent the apparent velocity in a region of no flow like in the medial temporo-occipital gyrus or anterior to the aqueduct in the midbrain) to correct eddy currents of brain motion but they have not detailed the relative value of the correction factor [2, 5].

Although there were no statistical differences between measurements using any of the two different approaches that correct the background offset, with consistent agreement between observers, background correction is important to reduce inaccuracies. To be noted, the midbrain background offset correction showed bigger difference between observers. Midbrain correction deviation is likely related to the ROI placed on the stationary tissue, as it is freely chosen by each observer. However, not every point of the brain suffers the same phase offset along the cycle. For these reasons, we may conclude that half-moon correction measures, being more reproducible, should be the one selected in CSF flow measurements.

**Fig. 4** Plot of the difference between measurements carried out by two observers using the *half-moon background correction*. Dotted line 95% confidence interval for agreement. **a** Measurements of mean stroke volume. **b** Measurements of mean flow

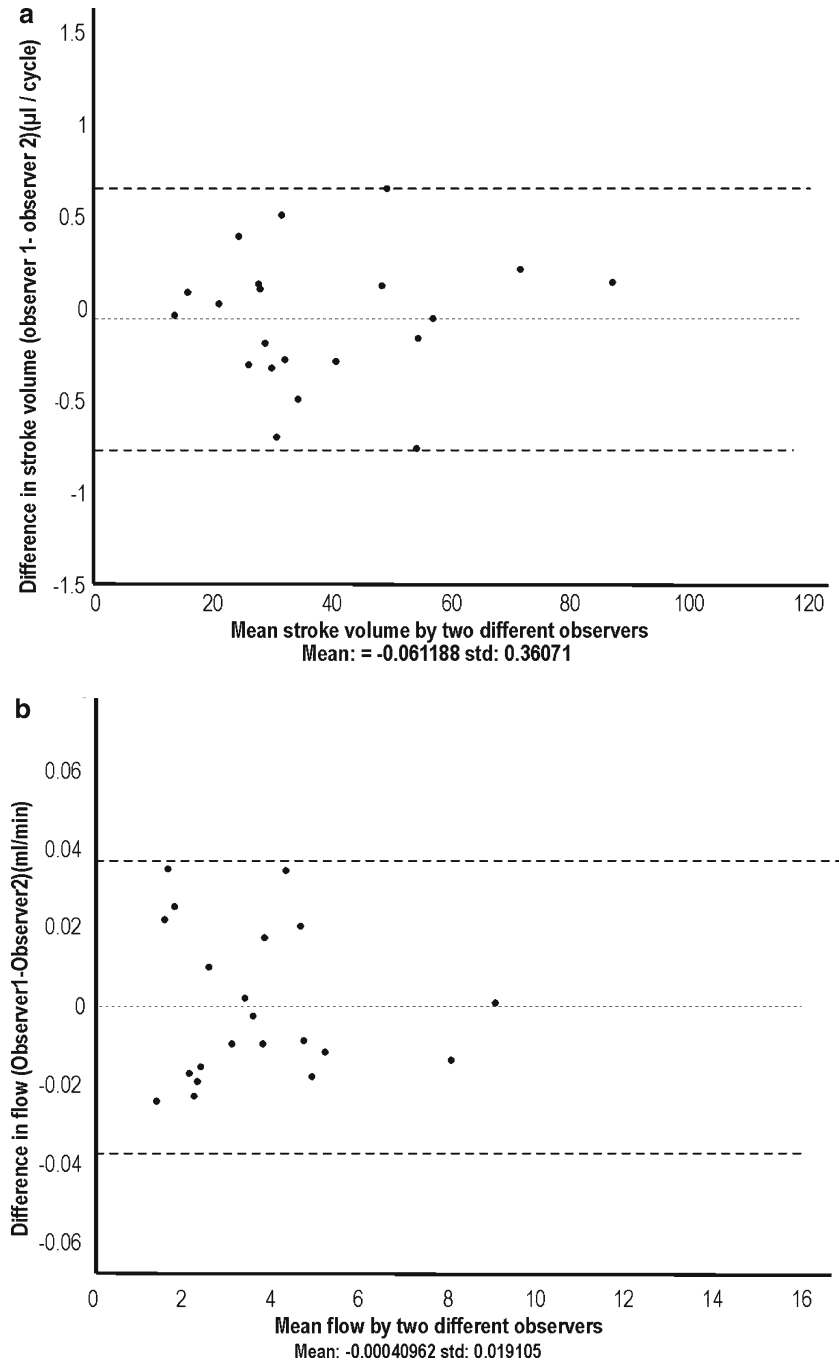


It was not necessary to apply an aliasing correction to any of the normal subjects' data of the present study due to the low flow velocities compared to the chosen velocity encoding although all subjects' data was completely analysed. Aliasing will surely be relevant in a clinical setting of patients with an increase flow dynamic.

Our velocity results for the maximal mean systolic velocity ( $5.27 \pm 1.3$  cm/s) and for the maximal mean dia-

stolic velocity ( $4.20 \pm 1.4$  cm/s) reflect some variability in comparison to previous studies [4, 26]. Lee et al. [4] obtained  $3.7 \pm 1.6$  cm/s for the peak systolic velocity while Marco et al. [27] obtained maximal values of  $4.5 \pm 1.9$  cm/s for systolic and  $4.0 \pm 1.9$  cm/s for diastolic velocities. Our slightly different values are most probably caused by the background correction and the semiautomatic ROI selection in our series.

**Fig. 5** Plot of the difference between measurements carried out by two observers using the *midbrain correction*. Dotted line 95% confidence interval for agreement. **a** Measurements of mean stroke volume. **b** Measurements of mean flow

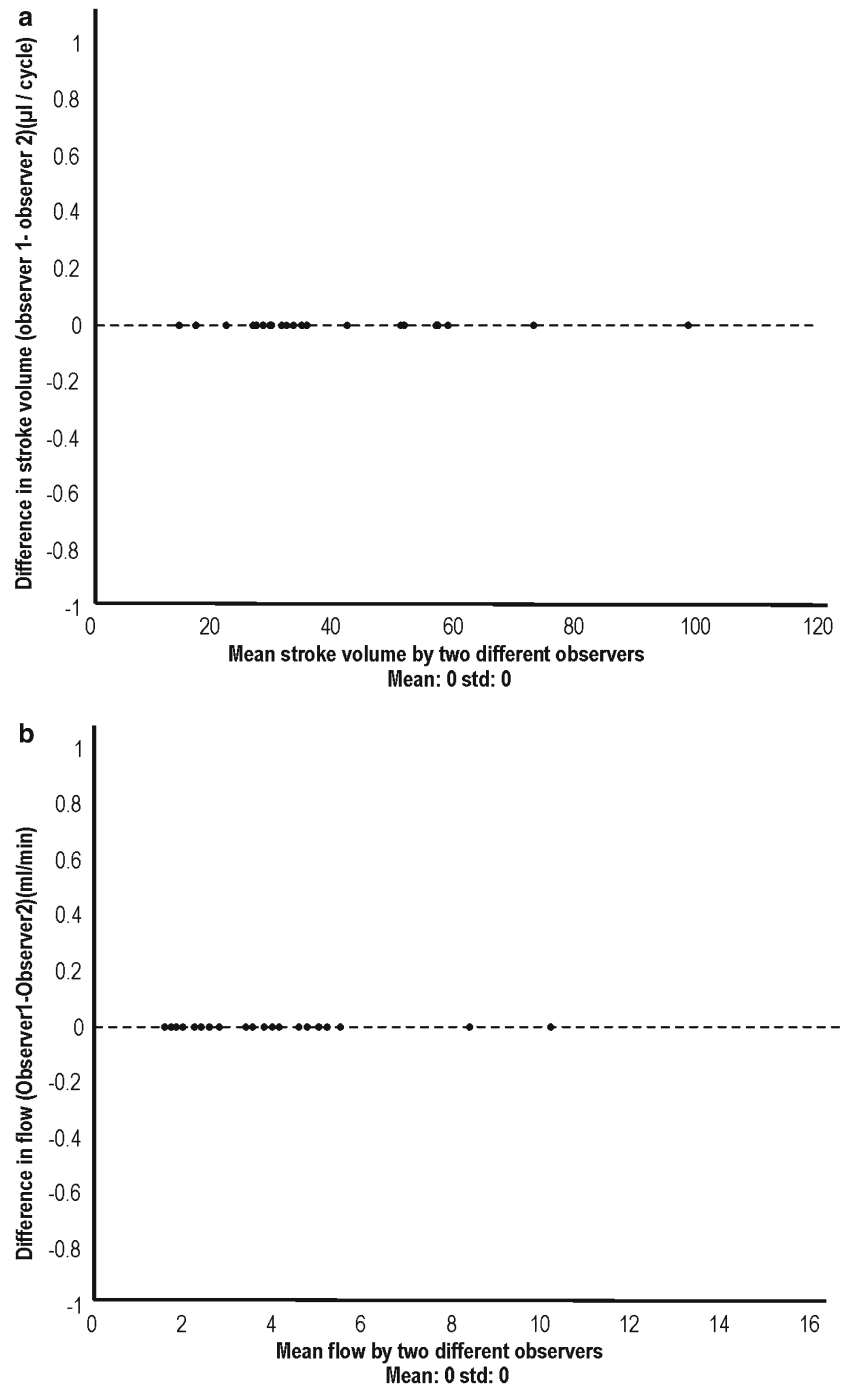


Our stroke volume values ( $39.19 \pm 20.13 \mu\text{l}/\text{cycle}$ ) are different in comparison to those obtained by Baledent et al. [12] ( $51 \pm 25 \mu\text{l}/\text{cycle}$ ) but closer to the values of Kim et al. [10] ( $30.1 \pm 19.8 \mu\text{l}/\text{cycle}$ ). The main difference with Baledent is probably due to the fact that we are measuring the stroke volume using a threshold to define the ROI and the background correction in order to reduce interobservers' variability and increase reproducibility calculated as half the difference between the maximum and the minimum mean intensity.

Previous studies of flow quantification [4, 11, 12], have used similar parameters obtaining favourable results. However, we recognize that the voxel size should be ideally less. Therefore, we have changed our acquisition protocol to a  $0.33 \times 0.33 \times 5 \text{ mm}$ . We hope to validate our method with this new approach in a large series of patients in the next months.

With the appropriate evaluation tools, cine MR flow quantification by means of phase contrast sequences provides a reliable tool to quantify pulsed CSF. A semi-

**Fig. 6** Plot of the difference between measurements carried out by two observers *without correction*. Dotted line 95% confidence interval for agreement. **a** Measurements of mean stroke volume. **b** Measurements of mean flow



automatic method (seed segmentation with half moon background and aliasing detection and correction) allows a generalization of the calculus of flow parameters with great consistency and independency of the operator.

**Acknowledgements** The authors would like to thank Dr. Norbert J. Pelc (Department of Radiology, Stanford University School

of Medicine, USA) for his constructive comments and helpful suggestions.

This work has been partially supported by the *CTBPRB/2004/342 FPI* grant of the *Generalitat Valenciana*, by the *IM3 Medical Imaging Net (Multimodal, Molecular and Medical Imaging)* and by a 2004–2005 *SERAM (Spanish Society for Medical Radiology)* grant.

## References

- Bradley WG, Scalzo D, Queralt J, Nitz WN, Atkinson DJ, Wong P (1996) Normal-pressure hydrocephalus: evaluation with cerebrospinal fluid flow measurements at MR imaging. *Radiology* 198:523–529
- Citrin CM, Sherman JL, Gangarosa RE, Scanlon D (1986) Physiology of the CSF flow-void sign – modification by cardiac gating. *Am J Neuroradiol* 7:1021–1024
- Pelc NJ (1995) Flow quantification and analysis methods. *Magn Reson Imaging Clin N Am* 3:413–424
- Lee JH, Lee HK, Kim JK, Kim HJ, Park JK, Choi CG (2004) CSF flow quantification of the cerebral aqueduct in normal volunteers using phase contrast cine MR imaging. *Korean J Radiol* 5:81–86
- Barkhof E, Kouwenhoven M, Scheltens P, Sprenger M, Algra P, Valk J (1994) Phase-contrast cine MR-imaging of normal aqueductal CSF flow – effect of aging and relation to CSF void on modulus MR. *Acta Radiol* 35:123–130
- Wolf RL, Ehman RL, Riederer SJ, Rossman PJ (1993) Analysis of systematic and random error in MR volumetric flow measurements. *Magn Reson Med* 30:82–91
- Bradley WG (1992) Magnetic resonance imaging in the evaluation of cerebrospinal fluid flow abnormalities. *Magn Reson Q* 8:169–196
- Bradley WG, Kortman KE, Burgoyne B (1986) Flowing cerebrospinal-fluid in normal and hydrocephalic states – appearance on MR images. *Radiology* 159:611–616
- Box FMA, Spilt A, Van Buchem MA, Van der Geest RJ, Reiber JHC (2003) Automatic model based contour detection and blood flow quantification in small vessels with velocity encoded magnetic resonance imaging. *Invest Radiol* 38:560–567
- Kim DS, Choi JU, Huh R, Yun PH, Kim DI (1999) Quantitative assessment of cerebrospinal fluid hydrodynamics using a phase-contrast cine MR image in hydrocephalus. *Childs Nerv Syst* 15:461–467
- Luetmer PH, Huston J, Friedman JA, Dixon GR, Petersen RC, Jack CR, McClelland RL, Ebersold MJ (2002) Measurement of cerebrospinal fluid flow at the cerebral aqueduct by use of phase-contrast magnetic resonance imaging: technique validation and utility in diagnosing idiopathic normal pressure hydrocephalus. *Neurosurgery* 50:534–542
- Baledent O, Feugeas MC, Peretti I (2001) Cerebrospinal fluid dynamics and relation with blood flow. A magnetic resonance study with semiautomated cerebrospinal fluid segmentation. *Invest Radiol* 7:368–377
- Kozerke S, Botnar R, Oyre S, Scheidegger MB, Pedersen EM, Boesiger P (1999) Automatic vessel segmentation using active contours in cine phase contrast flow measurements. *J Magn Reson Imaging* 10:41–51
- Yuan C, Lin E, Millard J, Hwang JN (1999) Closed contour edge detection of blood vessel lumen and outer wall boundaries in black-blood MR images. *Magn Reson Imaging* 17:257–266
- Alperin N, Lee SH (2003) PUBS: pulsatility-based segmentation of lumens conducting non-steady flow. *Magn Reson Med* 49:934–944
- Huang TY, Chung HW, Chen MY, Giang LH, BSC, Chin SC, Lee CS, Cheng CY, Liu YJ (2004) Supratentorial cerebrospinal fluid production rate in healthy adults: quantification with two-dimensional cine phase-contrast MR imaging with high temporal and spatial resolution. *Radiology* 233:603–608
- Enzmann DR, Pelc NJ (1992) Brain motion – measurement with phase-contrast MR imaging. *Radiology* 185:653–660
- Nitz WR, Bradley WG, Watanabe AS, Lee RR, Burgoyne B, Osullivan RM, Herbst MD (1992) Flow dynamics of cerebrospinal-fluid – assessment with phase-contrast velocity MR imaging performed with retrospective cardiac gating. *Radiology* 183:395–405
- Bhadelia RA, Bogdan AR, Wolpert SM (1995) Analysis of cerebrospinal-fluid flow wave-forms with gated phase-contrast MR velocity-measurements. *Am J Neuroradiol* 16:389–400
- Thomsen C, Ståhlberg F, Stubgaard M, Nordell B (1990) Fourier analysis of cerebrospinal fluid flow velocities: MR imaging study. *Radiology* 177:659–665
- Henk CB, Grampp S, Koller J, Schoder M, Frank H, Klaar U, Gomiscek G, Mostbeck GH (2002) Elimination of errors caused by first-order aliasing in velocity encoded cine-MR measurements of postoperative jets after aortic coarctation: in vitro and in vivo validation. *Eur Radiol* 12:1523–1531
- Frayne R, Rutt BK (1993) Frequency-response of retrospectively gated phase-contrast MR-imaging – effect of interpolation. *J Magn Reson Imaging* 3:907–917
- Greil G, Geva T, Maier SE, Powell AJ (2002) Effect of acquisition parameters on the accuracy of velocity encoded cine magnetic resonance imaging blood flow measurements. *J Magn Reson Imaging* 15:47–54
- Debatin JF (1998) MR quantification of flow in abdominal vessels. *Abdom Imaging* 23:485–495
- Chang LH, Chen CY, Chen MY, Huang TY, Chung HW (2000) Normal and abnormal cerebrospinal fluid dynamics evaluated by optimized cine phase-contrast MR imaging. *Chin J Radiol* 25:191–195
- Korosek FR, Turski PA (1997) Velocity and volume flow rate measurements using phase contrast magnetic resonance imaging. *Int J Neuroradiol* 3:203–318
- Marco G, Idy PI, Didon PA, Baledent O, Onen F, Feugeas MC (2004) Intracranial fluid dynamics in normal and hydrocephalus states. *J Comput Assist Tomogr* 28:247–254
- Bland JM, Altman DG (1986) Statistical methods for assessing agreement between two methods of clinical measurement. *Lancet* 327:307–310
- Prieto L, Lamarca R, Casado A (1998) Assessment of the reliability of clinical findings: the intraclass correlation coefficient. *Med Clin* 110:142–145
- Bartko J (1996) The intraclass correlation coefficient as a measure of reliability. *Psychol Rep* 19:3–11